

Proton Magnetic Resonance Study of Polycrystalline HCrO_2 JAMES A. IBERS, C. H. HOLM, AND C. R. ADAMS
Shell Development Company, Emeryville, California

(Received October 21, 1960)

A proton magnetic resonance study of polycrystalline HCrO_2 as a function of magnetic field and temperature is presented. HCrO_2 is paramagnetic, and electron paramagnetic dipole as well as nuclear dipole effects lead to line broadening. The lines are asymmetric and over the range of field $470 \leq H_0 \leq 9400$ gauss and temperature $77^\circ \leq T \leq 294^\circ \text{K}$ the asymmetry increases with increasing H_0 and decreasing T . An isotropic resonance shift of $\sim 0.03\%$ to lower applied fields indicates a weak isotropic hyperfine contact interaction. The general theory of resonance shifts is used to derive a general expression for the second moment M_{2p} of a polycrystalline paramagnetic sample and is specialized to HCrO_2 . The theory predicts a linear dependence of M_{2p} on $[H_0/(T+\theta)]^2$, where θ is the experimentally determined Curie-Weiss constant. The experimental second moment M_{2p}' conforms to the relation $M_{2p}' = (3.96 \pm 0.06) + (0.084 \pm 0.002)[H_0/(T+276)]^2$ in agreement with theory. Hence, the electron paramagnetic effects (slope) can be separated from the nuclear effects (intercept). The paramagnetic dipole effects provide some information on the particle shapes. The nuclear dipole effects provide some information on the motions of the hydrogen nuclei, but the symmetry of the O—H—O bond in HCrO_2 remains in doubt.

INTRODUCTION

THE magnetic moment of an unpaired electron associated nearby may have a tremendous influence on the magnetic resonance properties of nuclei. It is important to consider and experimentally verify this influence since quantitative nuclear resonance is becoming increasingly used in investigations of structure. HCrO_2 appeared to be well suited for the study of these matters, since it is a normal paramagnet, with three unpaired electrons on the chromium, its crystal structure is very simple, and the unknown position of the hydrogen in the strong O—H—O bond provides structural interest.

We first discuss the O—H—O bond in HCrO_2 . We then outline the theory of the interaction of paramagnetic dipoles with nuclei and show that the theory is in excellent agreement with experiment. Indeed it is possible to separate electron paramagnetic from nuclear effects. The information provided by the electron paramagnetic effects is then discussed, and finally the nuclear effects are interpreted in terms of various motional-modified models of the O—H—O bond in HCrO_2 .

O—H—O BOND IN HCrO_2

Theoretical studies of the hydrogen bond^{1,2} generally agree that the A—H—A bond will be linear in the absence of peculiarities of packing in the solid. Moreover, it will be asymmetric until a certain critical A—A distance is reached, below which it will become symmetric. There is ample evidence³ from many sources that the F—H—F bond in KHF_2 is symmetric. The F—F distance in KHF_2 is 2.26 Å.⁴ There is evidence,

though less convincing than for KHF_2 , that the O—H—O bond in nickel dimethylglyoxime is symmetric. Here the O—O distance is 2.44 Å.⁵ A number of semiempirical estimates by various workers^{1,2} lead to the conclusion that the O—H—O bond becomes symmetric when the O—O bond length is about 2.4 to 2.5 Å, but aside from the possible example of nickel dimethylglyoxime there have been no convincing reports of symmetric O—H—O bonds. Douglass⁶ has studied the crystal structure of HCrO_2 by x-ray diffraction. He finds the structure contains an O—H—O bond with the O—O distance of 2.55 ± 0.08 Å. There is, then, the possibility that this O—H—O bond is symmetric, although Douglass was unable to determine its symmetry from his x-ray data.

Douglass found HCrO_2 to be trigonal, Laue symmetry $\bar{3}m$, with $a = 4.787 \pm 0.005$ Å, $\alpha = 36.3 \pm 0.1^\circ$. X-ray and experimental density showed one formula unit in the unit cell, corresponding to a paramagnetic ion density of 0.029 Cr/Å³. The x-ray data did not permit Douglass to determine uniquely the space group, but a negative test for piezoelectricity led him to assume a center of symmetry. Under this assumption the space group must be $D_{3d}^5 - R\bar{3}m$ and the following are the positions of the atoms in the unit cell.⁷

Cr in 1(a): 0, 0, 0;

H in 1(b): $\frac{1}{2}, \frac{1}{2}, \frac{1}{2}$;O in 2(c): $\pm(x, x, x)$.

This space group requires the hydrogen bond to be symmetric. Douglass found powder intensity calculations and measurements to agree best for $x = 0.405$

¹ J. C. Slater, *Acta Cryst.* **12**, 197 (1959).² C. Reid, *J. Chem. Phys.* **30**, 182 (1959).³ See, for example, S. W. Peterson and H. A. Levy, *J. Chem. Phys.* **20**, 704 (1952).⁴ L. Helmholtz and M. T. Rogers, *J. Am. Chem. Soc.* **61**, 2590 (1939).⁵ L. E. Godycki and R. E. Rundle, *Acta Cryst.* **6**, 487 (1953).⁶ R. M. Douglass, *Acta Cryst.* **10**, 423 (1957).⁷ See, for example, *International Tables for X-ray Crystallography* (Kynoch Press, Birmingham, England, 1952), Vol. 1.

± 0.003 .⁸ These data lead to a structure in which sheets of Cr atoms lie between two sheets of O atoms. The O atoms in each sheet are close packed and each Cr atom is surrounded by a distorted octahedron of O atoms. The O—Cr—O layers are stacked normal to the [111] axis with the lower oxygens of one layer directly above the upper oxygens of the neighboring lower layer, in such a manner that the repeat is every three layers. The separate layers are joined together by hydrogen bonds. A drawing of the structure is to be found in reference 6.

The gross details of the structure appear reasonable. The structure appears to be unique among ROOH compounds, but is the same as that assumed by $\text{HNaF}_2(\text{NaHF}_2)$.⁹ The bond angles and distances are all within the expected limits and the volume per oxygen is about normal. However, the possible absence of a center of symmetry not only moves the hydrogen atom off $(\frac{1}{2}, \frac{1}{2}, \frac{1}{2})$, but also allows the oxygen atoms to become nonequivalent, with O_1 at (x_1, x_1, x_1) and O_2 at (x_2, x_2, x_2) (space group C_{3v}^5-R3m), where O_1 represents the oxygens on one side of the O—Cr—O layers and O_2 those on the other side. However, any oxygen non-equivalence would shorten either the already extremely short $\text{O}_1\text{—H—O}_2$ interlayer distance of 2.55 Å or the non-hydrogen-bonded $\text{O}_1\text{—O}_2$ interlayer interactions which are already quite short at 2.58 Å. Hence, it is difficult to conceive of a packing of the atoms in this material in which the oxygen atoms are far from geometrical equivalence. The only effect of lack of a center would then be to release the hydrogen atoms to occupy general, rather than special, positions along the [111] axis.

If the O—H—O bond is linear then there are three reasonable positions for the hydrogen atoms: (1) The hydrogen atoms are centered and hence all lie on a sheet midway between the oxygen sheets; (2) all hydrogen atoms lie on a sheet, but the sheet is closer to one oxygen sheet than to the other; (3) hydrogen atoms are asymmetrically placed, either randomly or in an ordered way, so that some hydrogen atoms are closer to the upper oxygen atoms while others are closer to the lower oxygen atoms. Position (2) appears to us to be unlikely in view of the absence of a piezoelectric effect and on general chemical structural grounds. A randomization of "ups" and "downs" is more likely than ordered "ups" and "downs" in position (3) since the hydrogen atoms are well separated and so the position of one could hardly affect the position of another, and also since ordered "up" and "down" implies a larger unit cell, for which no evidence exists. Therefore, the only unknown structural feature would appear to be whether the hydrogen atoms are located symmetrically (1) or asymmetrically (3).

⁸ Preliminary neutron diffraction results [W. C. Hamilton and J. A. Ibers (unpublished)] confirm this value of the oxygen parameter in HCrO_2 .

⁹ C. Andersen and O. Hassel, Z. physik. Chem. **123**, 151 (1926).

EXPERIMENTAL PROCEDURES

Samples

Douglass prepared his sample of HCrO_2 by thermal decomposition of aqueous chromic acid at 300–325°C. Dr. Douglass was kind enough to lend us about 5 grams of his material. This material proved to be unsatisfactory, since we could not obtain reproducible results on various portions of the sample. Subsequently, we learned from Douglass that his sample contained a few percent CrO_2 impurity. Since CrO_2 is ferromagnetic, we felt that any results obtained from the magnetically contaminated HCrO_2 would be suspect.

Plane¹⁰ suggested another preparation of HCrO_2 which we used here. 500 ml of 1M aqueous $\text{Cr}(\text{NO}_3)_3$ with 1 g CrO_3 added are heated in a bomb at 170°C for 48 hours.¹¹ A very fine, gray solid (about 15 g) is formed, water-washed by centrifugation, and dried at 110°C.

Differential thermal analysis showed a very small endothermic reaction at 340°C and a large endothermic reaction at 470°C. This latter reaction is in accord with the reported decomposition of HCrO_2 .^{12,13} Thermogravimetric analysis showed a weight loss of 1.8% centered at 337°C and another weight loss of 10.8% at 463°C. The expected weight loss for HCrO_2 going to H_2O and Cr_2O_3 is 10.6%. Mass spectrometric analysis of gases evolved upon heating to 410°C indicated nitrogen oxides and water vapor. The small reaction occurring at 337°C is probably caused by decomposition of occluded nitrates, and perhaps by a small amount of some hydrous material other than HCrO_2 . All subsequent measurements were made on material which had been heated to 375°C for one hour. Emission spectra indicated 0.01–0.1% calcium and all other impurities much lower. Chromium analysis gave 58.8% Cr as compared with 61.2% theory. However, HCrO_2 adsorbs water from the atmosphere and this may account for the low chromium analysis and high total weight loss.

The x-ray diffraction pattern of the material, taken with $\text{CuK}\alpha$ radiation, indicated the presence of no extra lines and was in good agreement with the pattern of Douglass. Magnetic analyses by R. G. Meisenheimer of this laboratory indicated no ferromagnetic impurities. HCrO_2 was found to be paramagnetic with three unpaired electron per chromium atom and a molecular susceptibility of

$$\chi(\text{HCrO}_2) = 3.20(T + \theta)^{-1} \times 10^{-24},$$

¹⁰ R. A. Plane, private communication, San Francisco American Chemical Society Meeting, April, 1958 (unpublished).

¹¹ J. Kumamoto of this laboratory has found that the yield of HCrO_2 is increased substantially if a small amount of isopropyl alcohol is added to the solution and if the bomb is heated at from 250° to 300°C overnight.

¹² A. W. Laubengayer and H. W. McCune, J. Am. Chem. Soc. **74**, 2362 (1952).

¹³ M. W. Shafer and R. Roy, Z. anorg. u. allgem. Chem. **276**, 275 (1954).

where $\theta = 276^\circ\text{K}$. For exactly three unpaired electrons the coefficient would be 3.10. An infrared spectrum, obtained by H. A. Benesi and R. G. Snyder of this laboratory, showed bands in the positions found by Jones.¹⁴

Electron microscopic examination of the HCrO_2 sample showed it to be composed of nearly isotropic particles about 0.3μ in diameter. The particles appeared rough and undoubtedly the single-crystal domains are smaller than this. The x-ray data are consistent with particle sizes of 1000 Å or greater. We found no obvious effects due to preferred orientation of the crystallites in this sample nor would we expect to on the basis of the shape found from electron microscopic examination.

Nuclear Magnetic Resonance (NMR) Measurements

The magnetic resonance absorption was detected by employing a Varian model V-4200 A broad line spectrometer and the associated 12-inch electromagnet system.^{15,16} One measurement at 40 Mc/sec was obtained with the Varian model V-4310 unit. A bridged- T type of bridge was used in the 10–16 Mc/sec range. The rf power level was maintained small enough at all times to prevent obvious line shape distortions by saturation effects. A modulation frequency of 40 cps with an amplitude as small as possible, commensurate with reasonably good signal-to-noise quality, was used. Background spectra were obtained in all cases. The spectrometer was adjusted to minimize the amount of dispersion mode mixed in with the absorption signal.

A single value of the thermal relaxation time T_1 at room temperature was measured by the progressive saturation method. The value of T_1 estimated at 470 gauss was 400 ± 200 microseconds. A single measurement of the spin-spin relaxation time T_2 was obtained at 10 Mc/sec by pulse methods. This measurement was obtained by W. Blumberg of the University of California, Berkeley, by observing the breadth of the free induction decay signal. The value derived was 16 microseconds.

Field shifts were derived from the mean value of the resonance line, defined as the field about which the first moment is zero.

Second moments of the spectra were computed by numerical integration. Corrections were applied for modulation broadening, apparatus background, and field shift.

Spectra were obtained over the temperature range of 77–294°K. For the low-temperature measurements the sample was cooled by a cold nitrogen gas flow method

similar to that of Andrew and Eades.¹⁷ The temperature was maintained to within about $\pm 2^\circ\text{C}$ for the period of time required to make the measurement (usually about one hour). One sample, which had been exposed to the atmosphere after evacuation at 375°C , showed the presence of adsorbed water (about 0.3 wt %) as evidenced by a weak resonance line which was very narrow at room temperature and which disappeared, due to broadening, at low temperature. The data reported here are either from spectra from which the adsorbed water resonance could easily be eliminated or from spectra of samples evacuated and sealed off at 375°C which contain no adsorbed water.

The measured powder density of the HCrO_2 used here was about 1.3 g/cm^3 , approximately one-third that of the crystal density (4.10 g/cm^3). Such a density corresponds to a paramagnetic ion density of about 0.01 Cr/\AA^3 .

Spectra were obtained from a powdered sample having the shape of a right circular cylinder with a height-to-diameter ratio of 4:1. The top of the sample was nearly flat and the bottom hemispherical. Spectra were also obtained from a sample in a spherical container which was made by blowing a bubble on the end of a capillary glass tube. The bubble was filled to the top and special precautions were taken to prevent any sample from remaining in the capillary. Spectra were also obtained from a third sample of HCrO_2 which had been diluted to three times its original volume with powdered, anhydrous alundum ($\alpha\text{-Al}_2\text{O}_3$). This sample was contained in a cylindrical container similar to that described above.

RESULTS AND DISCUSSION

General Considerations

In the absence of the electron magnetic moments and nuclear motion a symmetric proton resonance absorption line, whose features are determined solely by the equilibrium location of the nuclei, would be expected for HCrO_2 . However, for a fixed radio frequency ν each nucleus will absorb energy only when the total magnetic field at its location H satisfies the Larmor resonance condition $H = 2\pi\nu/\gamma$, where γ is the nuclear magnetogyric ratio. The effect of the large magnetic moment of the unpaired electron is to alter substantially the magnetic field at the nucleus from that of the external field. If we consider the instantaneous magnetic field at the proton nucleus in HCrO_2 , a calculation of the proton resonance linewidth would indicate several thousand gauss. Fortunately, however, in HCrO_2 as in other normal paramagnetic material the average lifetime of the electrons in their individual spin states is much shorter than the proton spin lifetimes in their respective states. Hence, the protons "see" only the static component of

¹⁴ L. H. Jones in a subsection of reference 6 above.

¹⁵ Varian Associates Instrument Division, Wide Line NMR Spectrometer V-4200B (Operating Manual).

¹⁶ A. K. Saha and T. P. Das, *Nuclear Induction* (Saha Institute of Nuclear Physics, Calcutta, 1957).

¹⁷ E. R. Andrew and R. G. Eades, Proc. Roy. Soc. (London) **A216**, 398 (1953).

the electron spin. This component is small compared with the instantaneous fields. For a single crystal of HCrO_2 all protons are equivalent¹⁸ and the effect of the chromium ions is to give a net shift to the whole spectrum equal to this static component. This static component is not uniform throughout space, since it results from the dipolar fields and the contact fields of the discrete chromium ions. These fields will, in general, be orientation dependent. Hence, the spectrum from a single crystal will be shifted a different amount for each orientation. A powder sample will therefore give a spectrum which is broadened, owing to the superposition of spectra shifted by various amounts. One would therefore expect that the spectra would broaden as the static electron magnetic moment increases. On the basis of dipolar effects alone, one would also predict an asymmetric line, with unshifted mean, since the shift for the individual crystallite should depend upon an asymmetric orientation function ($3\cos^2\chi - 1$). The effect of an isotropic contact field alone would be to give a uniform shift to the whole powder spectrum.

The experimental line shapes are in agreement with the above expectation. The lines possess a small isotropic shift and are, in general, asymmetric, the high-field wing being broader and flatter than the low-field wing. Both the shift and the asymmetry increase with increasing magnetic field and decreasing temperature. At the lowest field value used, viz., 470 gauss, and the highest temperature used, 300°K, the line shows very little asymmetry and possesses a shape which is more nearly Gaussian than Lorentzian in character.

Nuclear Resonance Shifts and Second Moments in Paramagnetic Crystals

We shall now consider the problem of second moments of resonance lines obtained for nuclei in paramagnetic crystals. Van Vleck¹⁹ has shown how the interaction of nuclear dipoles leads to line broadening and has derived in detail expressions for the second moment in terms of positions of the atoms. In this section we are concerned only with the additional broadening of the resonance line of powder samples as a result of the static magnetic fields of the electron moments.

The second moment M_2 of a resonance line about its mean value m is given by

$$M_2 = \langle (H - m)^2 \rangle = \langle H^2 \rangle - m^2, \quad (1)$$

where $\langle H^2 \rangle$ is the mean-square value of the resonance field distribution. It is apparent from (1) that M_2 is invariant to effects that simply shift the resonance to a new mean value leaving the distribution otherwise unaltered. For a single paramagnetic crystal m depends

upon the orientation of the crystal in the applied field. However, for fixed orientation the static electron moment leads only to a shift of the entire resonance, and the expression for M_2 , M_2^0 , will be the one derived by Van Vleck for the interaction of nuclear dipoles alone. The second moment for a powder sample M_{2p} is obtained, in the absence of preferred orientation effects, by an isotropic average of $\langle H^2 \rangle$ and m over all crystallite orientations:

$$\begin{aligned} M_{2p} &= \langle \langle H^2 \rangle \rangle_{\alpha, \varphi} - \langle m \rangle_{\alpha, \varphi}^2 \\ &= \langle M_2^0 \rangle_{\alpha, \varphi} + \langle m^2 \rangle_{\alpha, \varphi} - \langle m \rangle_{\alpha, \varphi}^2. \end{aligned} \quad (2)$$

In order to compute the paramagnetic contribution to M_{2p} , one needs an expression for the resonance mean as a function of crystal orientation.

McConnell and Robertson²⁰ have derived a general expression for nuclear magnetic field shifts of purely dipolar origin in paramagnetic molecules. Extending their results to include the effects of paramagnetic ions in a crystalline lattice and including the effects of the contact interaction, we find the mean of the resonance line for similarly situated nuclei to be

$$\begin{aligned} m &= H_0 - (g_{11}^2 \cos^2\alpha + g_{\perp}^2 \sin^2\alpha) C \left(\frac{H_0}{T + \theta} \right) \sum_j A_{ij} \\ &\quad - C \left(\frac{H_0}{T + \theta} \right) \sum_j r_{ij}^{-3} [g_{11}^2 \cos^2\alpha (3 \cos^2\chi_{ij} - 1) \\ &\quad + g_{\perp}^2 \sin^2\alpha (3 \sin^2\chi_{ij} \cos^2\varphi_{ij} - 1) \\ &\quad + \frac{3}{4} (g_{11}^2 + g_{\perp}^2) \sin 2\alpha \sin 2\chi_{ij} \cos \varphi_{ij}], \end{aligned} \quad (3)$$

where H_0 is the applied (z -directed) field and $C = |\beta|^2 S(S+1)(3k)^{-1}$, β is the Bohr magneton, S is the nuclear spin, and k is the Boltzmann constant. The first and second sums in (3) account for the contact and dipolar interactions, respectively. A_{ij} is the isotropic contact coupling constant, defined by the term $-A_{ij} \mathbf{u}_j \cdot \mathbf{u}_i$ ($\equiv \gamma \hbar |\beta| A_{ij} \mathbf{S}_j \cdot \mathbf{g} \cdot \mathbf{I}_i$) in the total spin Hamiltonian $\mathcal{H}_{\text{spin}}$, and $(3/8\pi)A_{ij}$ is the unpaired electron density $|\psi_j(0_i)|^2$ of ion j at nucleus i . The \mathbf{u} 's are magnetic moment vectors and \mathbf{g} is the electronic g tensor. In the derivation of the dipolar contribution to (3), the magnetic fields of the paramagnetic ions are considered as fields of point dipoles located at their respective lattice sites. Moreover, axial symmetry is assumed and g_{11} and g_{\perp} are the components of the electronic g tensor parallel and perpendicular to the figure axis. r_{ij} is the length of the vector joining i with j and making an angle χ_{ij} with the crystal axis. φ_{ij} measures the azimuthal orientation of \mathbf{r}_{ij} about the crystal axis and α defines the polar angle of the applied field relative to the crystal axis. A Curie-Weiss-formula-type approximation, $|E_{S_0}| \ll k(T + \theta)$, was used in determining the average (static) electron spin polarization.

¹⁸ This is strictly true only if the single crystal has the shape of an ellipsoid of revolution. In practice this condition is not usually fulfilled and nuclei that have different locations relative to the crystal boundary will see different static fields. The effect of this is to cause a slight broadening of the resonance lines.

¹⁹ J. H. Van Vleck, Phys. Rev. **74**, 1168 (1948).

²⁰ H. M. McConnell and R. E. Robertson, J. Chem. Phys. **29**, 1361 (1958).

E_{S_q} is the energy eigenvalue corresponding to the spin eigenvalue S_q and θ is an experimentally determined Curie-Weiss constant which is related to the exchange interaction among the electrons.

The mean value of the powder resonance m_p is obtained by averaging (3) over all orientations. Thus

$$m_p = \langle m \rangle_{\alpha, \varphi} = H_0 - \frac{C}{3} \left(\frac{H_0}{T + \theta} \right) \times [(g_{11}^2 + 2g_{12}^2)A + (g_{11}^2 - g_{12}^2)\Sigma], \quad (4)$$

where

$$A \equiv \sum_j A_{ij}, \quad \text{and} \quad \Sigma \equiv \sum_j r_{ij}^{-3} (3 \cos^2 \chi_{ij} - 1). \quad (5)$$

When we introduce (3) into (2) and perform the indicated averages, the second moment of the powder resonance becomes

$$M_{2p} = M_{2p}^0 + \frac{C^2}{45} \left(\frac{H_0}{T + \theta} \right)^2 \times [2(g_{11}^2 - g_{12}^2)A + (2g_{11}^2 + g_{12}^2)\Sigma]^2, \quad (6)$$

where M_{2p}^0 , the Van Vleck expression for the powder second moment resulting from the interaction of nuclear dipoles alone, is

$$M_{2p}^0 = \frac{3}{4} I(I+1) \gamma^2 \hbar^2 \sum_{i'} \langle r_{ii'}^{-6} (3 \cos^2 \theta_{ii'} - 1)^2 \rangle_{\alpha, \varphi} \quad (7)$$

$$= \frac{3}{5} I(I+1) \gamma^2 \hbar^2 \sum_{i'} r_{ii'}^{-6}. \quad (8)$$

The index i' accounts for the fact that here we are summing over nuclei. $\theta_{ii'}$ is the angle between the $\mathbf{r}_{ii'}$ and \mathbf{H}_0 .

The results expressed in (4) and (6) show that m_p and M_{2p} should vary linearly with $H_0/(T + \theta)$ and $[H_0/(T + \theta)]^2$, respectively, and that in the latter case the zero-field intercept is simply the Van Vleck expression for the second moment, in the absence of electron paramagnetism. It is clear, then, that in theory it is possible to separate the electron paramagnetic dipole interactions from nuclear dipole interactions in NMR experiments.

The second and third terms in (4) represent the isotropic contact shift and the pseudo contact shift, respectively. The pseudo contact shift results from the dipolar interactions and vanishes when $g_{11} = g_{12}$. For a material with isotropic g factor the shift of the mean value of the resonance is thus a measure of the strength of the isotropic contact interaction. On the other hand, the contact contribution to M_{2p} in (6) vanishes when $g_{11} = g_{12}$ and the slope of the linear plot becomes a measure of the strength of the dipolar interaction. In this latter case the slope of the linear plot may be written

$$\frac{1}{5} [\chi(T + \theta)\Sigma]^2, \quad (9)$$

where χ is the molecular susceptibility.

The dipole sum Σ is conditionally convergent and a sum out to the boundary determined by the sample container is required. In performing this sum the

effects of the distant dipoles are readily accounted for by bulk magnetization formulas,

$$\Sigma = \Sigma^0 + (\frac{4}{3}\pi - \eta)\rho + (\eta - \eta')\rho', \quad (10)$$

where Σ^0 is a finite dipole sum within a sphere of arbitrary radius centered at a measured nucleus; the sphere must be contained entirely within the crystallite. η is determined by the shape of the individual crystallites, and is equal to $4\pi/3$ if the crystallites are spherical and to 2π if they are cylindrical. η' is the analogous factor determined by the shape of the sample. ρ and ρ' are the paramagnetic ion densities in the crystallite and powder, respectively.

Dipole Sum and Shift Results for HCrO_2

In computing the dipole sum for HCrO_2 , the O—H—O bond is assumed symmetric. This is done for convenience since the dipole sum is relatively insensitive to the position of the H atom along the O—H—O bond. A displacement of the proton by 0.25 Å from the center along the bond reduces the dipolar sum by only 2%. A sum of the nearest 202 Cr ions contained within a sphere of diameter 24 Å gives $\Sigma^0 = 0.193 \text{ Å}^{-3}$. The value of Σ^0 oscillates between about 0.19 and 0.21 Å^{-3} as the diameter is increased. We arbitrarily chose 0.20 Å^{-3} as the value of Σ^0 . Using the paramagnetic ion density of 0.029 Cr/ Å^3 for the crystallite density of HCrO_2 , we obtain the value of $\Sigma = 0.20 + \frac{4}{3}\pi\rho = 0.32 \text{ Å}^{-3}$ as the dipole sum for a single crystal assumed infinite in all dimensions.²¹ Assuming the individual particles to be spherical, as indicated by the electron microscope study, and using the measured powder density of 0.01 Cr/ Å^3 , we obtain $\Sigma = 0.20 \text{ Å}^{-3}$ for the spherical sample used, 0.185 Å^{-3} for the undiluted cylindrical sample, and 0.195 Å^{-3} for the diluted cylindrical sample. This sum is rather insensitive to sample shape but quite sensitive to individual particle shape; this difference in sensitivity between particle and sample shape is due primarily to the difference in particle and powder densities. Measurements of the second moment, to be discussed below, indicate a spherical shape.

The g factor for most chromium compounds tends to be very nearly isotropic with an apparent value of about 1.98,²² very nearly that of a free electron. If we take a pessimistic viewpoint and let $g_{11} = 2.00$ and $g_{12} = 1.96$ as an extreme case of anisotropy, the expression for the shift, $\Delta H = m_p - H_0$, becomes

$$\Delta H = -[3.03A + 0.0411\Sigma]H_0/(T + \theta). \quad (11)$$

The shift of the resonance line was small compared

²¹ The dipole sum for an infinite (boundaryless) single crystal of HCrO_2 has also been computed by W. R. Heller of these laboratories using the Ewald method, which involves summing over both the real and reciprocal lattice. [See, e.g., M. H. Cohen and F. Keffer, Phys. Rev. **99**, 1128 (1955).] The value he obtains for HCrO_2 is 0.315 Å^{-3} .

²² J. D. Swalen of these laboratories has looked at the electron spin resonance of HCrO_2 and finds an apparent g factor of 1.976.

with the linewidth and could not be measured accurately. The results of several room-temperature measurements at about 3000 gauss are consistent with a shift of 1.0 ± 0.5 oersted toward lower applied fields.²³ The shift decreases as the applied field is reduced. If we use $\Sigma = 0.20 \text{ A}^{-3}$, this value of the shift leads to $A = 0.060 \text{ A}^{-3}$. Assuming a more realistic case of $g_{11} = g_{\perp} = 1.976$, we obtain

$$\Delta H = -3.07AH_0/(T+\theta), \quad (12)$$

for which $A = 0.062 \text{ A}^{-3}$. This isotropic contact shift factor is therefore rather insensitive to assumptions about the anisotropy of g and furthermore is quite small compared with the dipolar factor Σ . The values given above yield 0.0072 A^{-3} for the unpaired electron density at the hydrogen nucleus, $|\psi_{\text{Cr}}(0_{\text{H}})|^2$. Lack of knowledge of the crystal wave functions precludes a calculation to check this value, but it may be compared with an electron density of 0.087 A^{-3} which would result if the three unpaired electrons were uniformly distributed throughout the unit cell.

It should be emphasized that the quantity discussed here is the space-average shift. The shift for a particular crystal orientation is much larger than this, and it is this orientation-dependent shift which leads to a resonance line broadening. From the form of the shift expression in (4) one would predict a linear dependence of linewidth on $[H_0/(T+\theta)]$.

The spin-spin relaxation time T_2 may be estimated from the linewidth δH by using the relation $\delta H = 2(\gamma T_2)^{-1}$ which implies a Lorentzian line shape, when the spin-lattice relaxation time T_1 is long compared with T_2 .

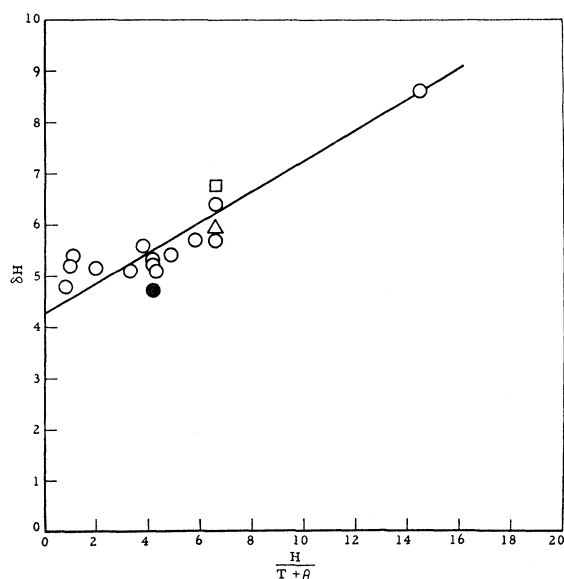


FIG. 1. The dependence of linewidth on temperature and field.

²³ The rather large error in the measured shift value may reflect in part a small admixture of dispersion mode in with the absorptive signal.

An estimate of 400 ± 200 microseconds for T_1 was obtained by the progressive saturation technique at 470 gauss and 295°C , while a value of 16 microseconds for T_2 at 2350 gauss and 295°C was obtained by pulse methods. The measured linewidth δH , defined as the separation in gauss between maximum and minimum on the derivative curve, is shown plotted against $H/(T+\theta)$ in Fig. 1. The scatter of the data reflects the uncertainty in measuring δH as a result of the flatness of the high-field wing of the derivative curve. The open circles represent data from the cylindrical, undiluted sample. The solid point in the figure represents the value of δH computed from the pulse measurement, while the triangle represents the result from the spherical sample. The square represents the linewidth for the cylindrical, diluted sample.

The sample shape, demagnetization, and bulk paramagnetism have no observable effect on the linewidth. Within the rather large experimental error in δH , the linewidth appears to be a linear function of the static electron magnetic moment in HCrO_2 , in qualitative agreement with the prediction of Eq. (4). In view of the large uncertainty in linewidth measurements and the much more reliable second moment data below, no quantitative calculations from the linewidths were made.

Second Moments of HCrO_2

The experimental (primed) second moments are shown in Fig. 2 as a function of $[H_0/(T+276)]^2$. A least-squares fit of the data to a straight line gives

$$M_{2p}' = (3.96 \pm 0.06) + (0.084 \pm 0.002)[H_0/(T+276)]^2. \quad (13)$$

The exceedingly good fit of this line to the data is all the more remarkable when one notes that the 40-Mc/sec point (upper right-hand corner) was not used in the least-squares analysis and yet falls essentially on the extrapolated straight line.

When we perform the indicated sums²⁴ in (6) for a symmetric hydrogen bond, let $g_{11} = 2.00$ and $g_{\perp} = 1.96$ as an extreme case of anisotropy for HCrO_2 , and use the values of Σ and A given in the section above, then Eq. (6) becomes

$$M_{2p} = 3.63 + 0.077[H_0/(T+\theta)]^2. \quad (14)$$

If we assume the more realistic case of $g_{11} = g_{\perp} = 1.976$, we find the slope to be 0.075. The slope calculated from the experimental susceptibility [Eq. (9)] is 0.082.

In the treatment above we have assumed the lattice to be rigid. The zero-point motions of the nuclei will affect the dipole sum and hence the theoretical slope. We have considered, in a manner analogous to that discussed below concerning the effect of motion on the zero-field second moment, the effects of motion of the

²⁴ We neglect the contribution to M_2 of the Cr^{53} nucleus, for this contribution is less than 0.1%.

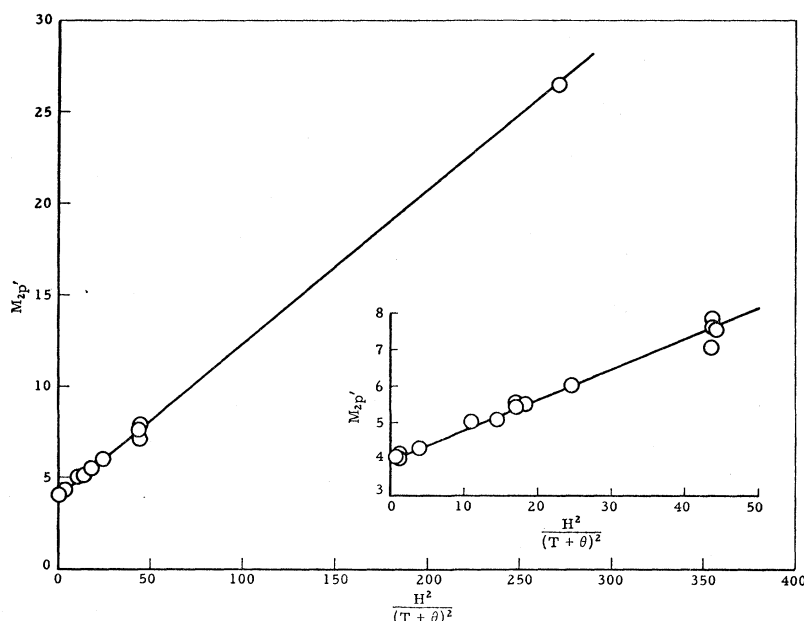


FIG. 2. The dependence of second moment on temperature and field. ($\theta = 276^\circ\text{K.}$)

hydrogen nucleus on the contributions to the dipole sum of the six nearest hydrogen-chromium interactions. We find that these contributions are increased by about 3%. It seems likely that the effects of the hydrogen motion on the remaining contributions will tend to cancel out when summed. Hence, the theoretical slope will be increased by at most about 6% as a result of zero-point motion.

In Table I we summarize the theoretical values of the slope obtained from the various equations on the assumption that $\Sigma = 0.20 \text{ \AA}^{-3}$. The agreement with the experimental value of 0.084 ± 0.002 (deg-oersted/gauss)² is remarkable. This agreement is even more remarkable when one considers that the calculations were made on the basis of a point dipole approximation for the chromium ions rather than a dipole distributed over the chromium *d*-electron wave functions. Since Σ changes markedly as the particles deviate from sphericity, this agreement confirms the approximately spherical shape of the particles.²⁵

The errors involved in the dipole sum, and hence in the theoretical slopes, arising primarily from shape and

motion effects, preclude, even if the *g* factors were known with certainty, comparison with the experimental slope to yield information of structural interest, e.g., the position of the hydrogen atom along the O—H—O bond.

Interpretation of the Zero-Field Second Moment

The lack of agreement between the theoretical M_{2p}^0 (3.63 oersteds² for the case of a symmetric O—H—O bond) and experimental $M_{2p}^{0'}$ (3.96 oersteds²) values of the intercept requires further explanation. We need only consider Van Vleck's expression for the second moment [Eq. (7)] which involves the interaction among the protons. In treating the problem of second moments, we have ignored the off-diagonal elements of $\mathcal{H}_{\text{spin}}$. Bloembergen, Purcell, and Pound²⁶ have shown that these terms are effective in second order for allowing interchange of thermal energy between the spin system and the lattice and thereby contribute to the lifetime of the individual spin state. The effect of a short T_1 is to broaden the resonance line by folding in a component having Lorentzian character. We assume that the enhanced broadening is equivalent to the characteristic breadth (between points of inflection) of a collision broadened Lorentz line, viz., $(\sqrt{3}\gamma T_1)^{-1}$. The net resultant average lifetime of the spins is thus given by

$$1/T_2 = 1/T_2' + 1/2\sqrt{3}T_1, \quad (15)$$

where T_2' is the lifetime determined solely by the diagonal elements of $\mathcal{H}_{\text{spin}}$. The effect of T_1 on the second moment is to make the experimental value too large. If we assume a Gaussian line shape, in agreement

TABLE I. Values of the theoretical slope.

g_{11}	g_{\perp}	$\chi(T+\theta) \times 10^{24}$	Slope (rigid)	Slope (motion)
2.00	1.96	...	0.077	0.083
1.976	1.976	...	0.075	0.079
...	...	3.20 ^a	0.082	0.087

^a Experimental value.

²⁵ By particles we here mean those domains whose average density is essentially that of a single crystal; this differs markedly from the powder density. It is not necessary that these particles be single crystals.

²⁶ N. Bloembergen, E. M. Purcell, and R. V. Pound, Phys. Rev. 73, 679 (1948).

with the observations for HCrO_2 at low fields, then $(\gamma T_2')^{-2}$ is the second moment we wish to compare with theory and not an experimentally measured value $(\gamma T_2)^{-2}$. For comparison with theory it is required therefore that the experimental second moment be changed by a factor of about $[1 - (T_2/2\sqrt{3}T_1)]^2$. In order to obtain agreement between the experimental moment, 3.96 oersteds², and the rigid lattice value, 3.63 oersteds², T_1 must be about 100 μsec . This is lower than the value 400 ± 200 μsec found for T_1 . Furthermore, T_1 for nuclei in paramagnetic materials should be strongly temperature dependent,²⁷ increasing with decreasing temperature. Since we did not observe any temperature dependence, other than the static dipolar effect, we must conclude that T_1 is already quite long even at room temperature. It is clear, then, that the discrepancy between the second moments cannot be due to T_1 effects. On the other hand, the value of the calculated second moment has been derived on the assumption that the lattice is rigid.

Van Vleck's formula, Eq. (7), for the rigid lattice nuclear dipole-dipole second moment of the resonance line must be modified to take account of the nuclear motions arising from zero-point energy. [The consistency of room-temperature and low-temperature results (Fig. 2) clearly indicates that motional effects arising from other than zero-point energy terms may be neglected.] If these nuclear motions are of frequencies great compared with the linewidth frequency (for example, if they are in the infrared), the appropriate modification of Van Vleck's expression is

$$M_{2p}^0 = \frac{3}{4} I(I+1) \gamma^2 \hbar^2 \times \sum_{i' \neq i} \langle ((3 \cos^2 \theta_{ii'} - 1) r_{ii'}^{-3})_{\text{motion}} \rangle_{\text{space}} \\ = c_i \sum_{i' \neq i} \langle (U_{ii'})_{\text{motion}} \rangle_{\text{space}}. \quad (16)$$

It is not possible to write down a complete description of the motions of the nuclei in a crystal of HCrO_2 , and certain approximations must be adopted. In addition, since the positions of the hydrogen atoms are not known with certainty, it is impossible to use the disparity between the experimental second moment (i.e., the intercept of Fig. 2), and the rigid-lattice second moment to evaluate directly the amplitudes of motion of the nuclei. Rather we shall examine the consequences of assuming certain hydrogen atom configurations on the amplitudes necessary to eliminate this disparity, and by comparison of these amplitudes with those obtained in other studies evaluate the reasonableness of the assumed configurations.

Previous experience with motional corrections in the case of the ammonium ion,²⁸ where a comparison of the various approximations with a more precise normal co-

ordinate treatment was possible, led us to adopt here, without formal justification, rather similar approximations. The first one is that the motions of the hydrogen nuclei in HCrO_2 are uncoupled. The second assumption is that the proton motion may be described by a stretching vibration along the O—H—O bond and by two mutually perpendicular bending frequencies normal to this bond. These two assumptions were used successfully for the ammonium ion,²⁸ and there the case for uncoupled motion of the protons is far less secure. The amplitudes of vibration are small compared with the bond length, and so we assume that the bending vibrations are normal to the bond, rather than that they are executed in arcs. This assumption makes the algebra tractable. In addition, we assume that motion affects only the nearest proton-proton contributions to the second moment. These contributions amount to about 85% of the total moment, and so the relative correction to these contributions should be quite close to the relative correction to the total moment.

We take the O—H—O bond to be parallel to the z axis, one proton H_1 , without motion, at (0,0,0) and another proton H_2 at (0, a , b) in the absence of motion. $b/2$ is the displacement of the proton from the symmetric position. The term in the second moment for this pair becomes

$$\langle \langle (U_{H_1 H_2})_{\text{motion}} \rangle^2 \rangle_{\text{space}} \\ = U_{H_1 H_2}^0 \left[1 + \frac{12}{(a^2 + b^2)^2} (2b^2 - a^2) (\langle \delta r_s^2 \rangle - \langle \delta r_B^2 \rangle) \right], \quad (17)$$

where

$$U_{H_1 H_2}^0 = \frac{4}{5} (a^2 + b^2)^{-3}, \quad (18)$$

and where $\langle \delta r_s^2 \rangle$ and $\langle \delta r_B^2 \rangle$ are the mean-square amplitudes of the stretching and bending vibrations, respectively. There is evidence²⁹ that the O—H distance increases as the O—O distance decreases, and with a knowledge of systems with similar O—O distances (where the O—H distance is known) we assume an O—H of 1.05 Å. If we take the O—O distances as 2.55 Å, the O—H of 1.05 Å leads to $b = 0.44$ Å. From the crystal structure $a = 2.984$ Å. This gives

$$M_{2p}(\text{opposed}) = c_H \langle \langle (U_{H_1 H_2}) \rangle^2 \rangle \\ = 0.474 [1 + 1.23 \Delta], \quad (19)$$

where

$$\Delta = \langle \delta r_B^2 \rangle - \langle \delta r_s^2 \rangle, \quad (20)$$

and the notation $M_{2p}(\text{opposed})$ represents the contribution to the second moment (in oersteds²) for a pair of protons each of which is closest to a different sheet of oxygens. If $b = 0$ (protons in the symmetric position) or if both protons are closest to the same sheet of oxygens,

$$M_{2p}(\text{adjacent}) = 0.507 [1 + 1.35 \Delta]. \quad (21)$$

²⁷ R. G. Shulman and V. Jaccarino, Phys. Rev. **108**, 1219 (1957).
²⁸ J. A. Ibers and D. P. Stevenson, J. Chem. Phys. **28**, 929 (1958).

²⁹ See, for example, Table II of C. G. Shull and E. O. Wollan, *Solid State Physics*, edited by F. Seitz and D. Turnbull (Academic Press, Inc., New York, 1956), Vol. 2.

TABLE II. Thermal motions of hydrogen atoms from neutron diffraction data.

Substance	Ref.	$A-A$, Å	$\langle \delta r_B^2 \rangle$, Å ²	$\langle \delta r_S^2 \rangle$, Å	Δ	$\langle \delta r^2 \rangle$
Ca(OH) ₂	30	...	0.054	0.017	0.037	
(C ₆ H ₅ CH ₂ COO) ₂ KH	31	2.54	$\delta r_B^2 \geq \delta r_S^2$		~0	0.084
KH ₂ PO ₄	32	2.49	0.029	0.082	-0.053	
Na ₂ CO ₃ ·NaHCO ₃ ·2H ₂ O	33	2.50	$\delta r_B^2 < \delta r_S^2$		<0	0.049
KHF ₂	3	2.26			~0	0.012

We pointed out earlier that the two possible configurations for the hydrogen atoms in HCrO₂ which we would hope to choose between are the symmetric (centered) configuration and the random (noncentered) configuration. The six nearest-neighbor proton-proton interactions in HCrO₂ are all equivalent if the proton is symmetrically placed so

$$M_{2p}(\text{symmetric}) = 6M_{2p}(\text{adjacent}) \\ = 3.04(1 + 1.35\Delta). \quad (22)$$

On the other hand, in the random, asymmetric model a given proton on the average will have three closest neighbors "adjacent" and three "opposed" and so

$$M_{2p}(\text{random}) \\ = 3(M_{2p}[\text{opposed}] + M_{2p}[\text{adjacent}]) \\ = 2.94(1 + 1.29\Delta). \quad (23)$$

We assume that the motional corrections for the more distant interactions are negligible. The contributions to the second moment of these non-nearest-neighbor interactions amount to 0.59 oersted² for the symmetric model and, to a good approximation, the same in the random model. We may therefore subtract 0.59 from the experimental value of 3.87 (which has been corrected approximately for T_1 effects) and obtain 3.28 to compare with theory, including motion. Accordingly, we obtain

$$\Delta(\text{symmetric}) = 0.058 \text{ Å}^2, \quad (24)$$

$$\Delta(\text{random}) = 0.090 \text{ Å}^2. \quad (25)$$

If we had assumed an O—H of 1.00 Å, we would have obtained $\Delta(\text{random}) = 0.11 \text{ Å}^2$.

Some results on thermal motions^{3,30-33} which are typical of those found in neutron diffraction studies of hydrogen-containing substances are shown in Table II. There is no hydrogen bonding in Ca(OH)₂ and the Δ is positive. The F—H—F bond in KHF₂ is symmetric; the Δ is approximately zero and the mean amplitude of vibration small. The Δ in potassium hydrogen bisphenylacetate is approximately zero, but the mean amplitude of vibration of the hydrogen atom is large. In KH₂PO₄ and in sodium sesquicarbonate the Δ 's are negative. Although these data indicate no clear trends

of value in choosing between the symmetric or asymmetric configurations in HCrO₂, by their discordance they indicate that the thermal motions demanded by (24) or (25) are not unreasonable.

The results of (24) and (25) do give some information which was not evident *a priori*. A symmetric hydrogen bond could be interpreted in two ways: (1) by a single minimum in a symmetric potential function, or (2) by rapid tunneling through a barrier separating two minima of equal depth at equal distances from the center. This second interpretation can be safely eliminated on the basis of the observed positive Δ : The tunneling would result in an effective stretching amplitude much greater than the bending amplitude and Δ would be negative. Tunneling is probably the explanation for the negative Δ 's in Table II. Tunneling, if it exists in HCrO₂, must occur at a frequency lower than the frequency equivalent of the proton resonance linewidth (about 17 kc/sec).

It must be recalled that we have assumed here that the O—H—O bond is linear. Results similar to those derived above would apply if the bond were assumed to be nonlinear. Clearly more data are needed before the nature of the O—H—O bond in HCrO₂ can be understood. These resonance results are complementary to infrared and neutron diffraction data, and it is possible that a combination of information from these diverse methods may eventually lead to an unequivocal picture of the hydrogen bond in HCrO₂ and hence to a better understanding of hydrogen bonding in general.

SUMMARY AND CONCLUSIONS

The dependence of the second moment of the proton resonance of polycrystalline HCrO₂ on applied field and absolute temperature has been interpreted on the basis of electron-nuclear as well as nuclear-nuclear point dipole interactions. The general theory of resonance shifts²⁰ has been extended to the calculation of second moments of powder samples, and excellent agreement between theory and experiment has been obtained. Some of the conclusions are:

(1) The line shape is asymmetric, with asymmetry increasing with increasing H_0 and decreasing T .

(2) The resonance shift is proportional to $H_0/(T+\theta)$, where θ is the experimentally determined Curie-Weiss constant and is related to the exchange interaction among the electrons. The proportionality constant is a function of both the contact interaction and the pseudo

³⁰ W. R. Busing and H. A. Levy, J. Chem. Phys. **26**, 563 (1957).

³¹ G. E. Bacon and N. A. Curry, Acta Cryst. **10**, 524 (1957).

³² G. E. Bacon and R. S. Pease, Proc. Roy. Soc. (London) **A220**, 397 (1953); **A230**, 359 (1955).

³³ G. E. Bacon and N. A. Curry, Acta Cryst. **9**, 82 (1956).

contact interaction; both of these interactions involve the anisotropy of the electronic g factor. The former interaction involves the Fermi constant A ; the latter interaction involves the paramagnetic dipole sum Σ computed at a nuclear lattice site, and vanishes when g is isotropic (i.e., $g_{11} = g_{\perp}$).

(3) M_{2p} varies linearly with $[H_0/(T+\theta)]^2$, the slope and zero-field intercept arising from the interactions of the electron-nuclear dipoles and the nuclear-nuclear dipoles, respectively. In principle, therefore, it is possible to effect a complete separation of these interactions. The zero-field intercept is interpretable in terms of the Van Vleck¹⁹ theory which is usually applied to diamagnetic materials. The slope, on the other hand, is related in a complex fashion to the Fermi contact interaction, the dipole sum, and the g -factor anisotropy.

It is desirable to be able to separate the A , Σ , and g effects discussed above, for a knowledge of A and g -factor anisotropies can give precise information about the paramagnetic-ion crystal wave functions. Σ depends upon the crystal structure, particle and sample shapes, and nuclear motions. In general, more information is required to make a complete separation of A , Σ , and g than can be obtained from the measurements of (2) and (3) above. Additional information might be obtained, for example, from studies involving single crystals.

For HCrO_2 the results conform to the theoretical predictions above. The shift, however, is very small, indicative of a nearly isotropic electronic g factor (i.e., $g_{11} \cong g_{\perp}$) and a very weak contact interaction. On the assumption that $g_{\perp} = g_{11}$ we derive a value of Σ from the experimental slope of M_{2p}' vs $[H_0/(T+\theta)]^2$ that agrees remarkably well with that computed using the known crystal structure and certain reasonable

assumptions about the particle shape and about the positions and zero-point energy motions of the hydrogen nuclei. The theoretical slope for HCrO_2 is rather insensitive to the location of the hydrogen along the O—H—O bond so that despite the excellent agreement between theory and experiment we were unable to learn anything about the symmetry of this bond from the slope measurements. On the other hand, the theoretical slope is a very sensitive function of the assumed partial shape, and the agreement between theory and experiment confirms the reasonableness of the particle shape we assumed.

The nuclear dipole second moment (i.e., that value obtained from the zero-field intercept) did not allow us to distinguish between a symmetric or asymmetric O—H—O bond in HCrO_2 , but it did allow us to eliminate a model of the bond in which there is rapid tunneling of the hydrogen atom between two equilibrium positions. In addition, information was obtained on the amplitudes of vibration of the hydrogen nuclei.

At extremely low fields we would expect the theory presented here to be inadequate, for it does not take account of exchange interaction between nuclei and the electrons. It may be possible to derive information on such exchange from measurements of second moments and shifts at very low fields.

ACKNOWLEDGMENTS

We wish to acknowledge many fruitful discussions with our colleagues, in particular with W. R. Heller and J. D. Swalen. We wish to thank R. G. Meisenheimer for the magnetic measurements, H. A. Benesi and R. G. Snyder for the infrared measurements, and W. Blumberg for the pulsed measurement of T_2 .